Measurement of the linear polarization of channeling radiation in silicon and diamond

M. Rzepka, G. Buschhorn, E. Diedrich, R. Kotthaus, W. Kufner, W. Rössl, and K. H. Schmidt
Max-Planck-Institut für Physik (Werner-Heisenberg-Institut), 80805 München, Germany

P. Hoffmann-Stascheck, H. Genz, U. Nething, and A. Richter
Institut für Kernphysik, Technische Hochschule Darmstadt, 64289 Darmstadt, Germany

J. P. F. Sellschop
University of the Witwatersrand, 2050 Johannesburg, South Africa
(Received 13 February 1995)

Utilizing 90° Compton scattering the linear polarization of channeling radiation produced at the superconducting accelerator S-DALINAC with 62 MeV electrons in silicon and diamond has been measured in the energy range between 50 and 400 keV. Planar channeling radiation due to transitions involving transversal bound as well as unbound states is completely linearly polarized perpendicular to the channeling plane. Axial channeling radiation does not show linear polarization.

I. INTRODUCTION

Channeling radiation[1] is emitted when relativistic electrons traverse a crystal very close to a main axis or plane. The radiation is due to spontaneous transitions between bound states of the transversal electron motion in the potential generated by the strings or planes of ions. Spectral properties of channeling radiation have been studied extensively[2] and are well described by potential model calculations based on the "many-beam" formalism introduced by Andersen *et al.*[3] Planar channeling radiation emitted in the forward direction is predicted[4–6] to be completely linearly polarized perpendicular to the channeling plane. In contrast, axial channeling radiation emitted in the exact forward direction is expected not to be linearly polarized as there is azimuthal symmetry. Possible circular polarization is not detectable with our experimental method. Off axis, there may be linear polarization components.[3,7,8]

The linear polarization of planar channeling radiation of a few MeV produced in a diamond crystal by electrons of about 1 GeV was measured by Adishchev and coworkers.[9,10] At such high energies individual transitions between transverse bound states cannot be resolved any more. Recently, we have published experimental results on linear polarization of planar channeling radiation produced by 65 MeV electrons in silicon in the energy range up to 200 keV which is dominated by discrete lines due to transitions between bound states.[11] The measurements revealed a high degree of linear polarization.

The purpose of the measurements reported here is a high precision study of linear polarization of planar and axial channeling radiation in silicon[7] and diamond[12] using an improved apparatus and refined analysis procedures. In all experiments, Compton scattering under 90° was employed as the analyzing process. In Ref. 11 the scattering plane was fixed and yield asymmetries were measured for equivalent channeling planes oriented parallel and perpendicular to the scattering plane, respectively. In the present experiments, we measured complete azimuthal angular distributions of Compton scattered channeling radiation produced for a given crystal orientation. This method allows us to also probe the polarization of axial channeling radiation and to determine the orientation of the polarization plane. Furthermore, it is insensitive to possible slight differences in the horizontal and vertical beam divergences. Some preliminary results have been presented earlier.[13]

II. EXPERIMENTAL SETUP

A. Electron beam and channeling setup

The experiment (Fig. 1) was carried out at the superconducting electron linear accelerator S-DALINAC.[14] An uncollimated cw beam of (62 ± 0.3) MeV electrons has been steered onto the crystal mounted on a goniometer in a vacuum chamber. Typical beam currents for polarization analysis were a few hundred nA whereas spectra of forward going channeling radiation were taken at beam currents of the order of one nA. The beam spot size, position, direction and divergence were measured and monitored by means of two retractable fluorescence screens ($L1$ and $L2$ in Fig. 1) 5.4 m apart positioned up- and downstream the channeling crystal. The beam was focused to a diameter of 2 to 3 mm and a divergence of less than 0.6 mrad which is smaller than the critical channeling angle ($\varphi_c = 0.8$ mrad) typical for the conditions of these experiments. After leaving the crystal the electrons were deflected by 40° using a system of dipole magnets denoted $M1$ to $M3$ in Fig. 1.

The radiation produced by the channeling process in the crystal has been detected in forward direction by means of a germanium detector about 9 m downstream of the crystal. The detector was located behind a 1.6 m thick concrete shielding wall and an additional lead shielding with a total thickness of 30 cm. At the far end

0163-1829/95/52(2)/771(7)/$06.00 ©1995 The American Physical Society

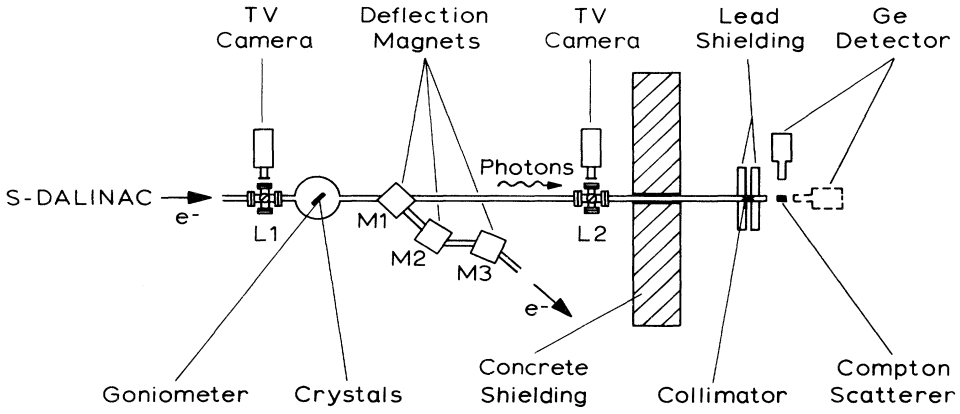

FIG. 1. Schematic view of the experimental setup. The high-purity germanium detector is indicated both in the position to measure forward going radiation (with the polyethylene Compton scatterer removed) and at 90° to measure Compton scattered radiation. The distance between crystal and detector amounts to around 9 m. The two fluorescence screens $L1$ and $L2$ are 5.4 m apart.

the vacuum beam tube was sealed by a 50 μm thick Kapton foil. The acceptance of the photon detector was limited to 1.2×10^{-6} sr by means of a lead collimator aligned with the direction of the undeflected electron beam within 0.2 mrad.

B. Crystals and goniometer

Two crystals were used in these experiments, a 13 μm thick silicon crystal ($Z=14$) cut perpendicular to the $\langle 100\rangle$ axis and a 50 μm thick natural diamond crystal ($Z=6$) cut perpendicular to the $\langle 110\rangle$ direction. Both crystals were mounted simultaneously on a two axes, two translations goniometer. The angular step width of 0.175 mrad was well below the typical critical channeling angle $\varphi_c\approx0.8$ mrad. The translational step width of the goniometer was 1 μm with a total range of 50 mm both in the vertical and horizontal directions. This allows one to move the crystal out of the electron beam and to control the beam spot at any time desired.

C. Photon detector and read out

Energy spectra of channeling radiation were measured using an intrinsic high-purity coaxial germanium detector. The detection efficiency as determined from bremsstrahlung spectra taken with the silicon crystal in random orientation peaks around 170 keV and drops steeply below 100 keV. We restricted our analysis to photon energies above 50 keV where the detection efficiency is at least 20% of the peak value. The detector signal was processed by amplifiers and digitized by a 10 bit CAMAC ADC. The digital data were transferred via general purpose interface bus (IEEE 488) to a Personal Computer.

D. Compton polarimeter

For the polarization measurements a cylindrical 54 mm long polyethylene target (5.08 g/cm^2) of 25 mm diameter was used for 90° Compton scattering. To measure energy spectra of the Compton scattered photons the photon detector was mounted on a vertical turntable perpendicular to the incident photon direction at a distance of 140 mm from the scattering target (see Fig. 2). It covered an angular range of $\Delta\varphi=190°$, such that the complete azimuthal angular distribution of Compton scattering yields could be measured.

III. METHOD

A. Crystal alignment

The crystal was oriented by angular scans of the fractional photon yield within the energy interval containing the main transition lines (75 to 170 keV and to 250 keV for forward channeling radiation in silicon and diamond, respectively; 65 to 140 keV and to 170 keV for 90° Compton scattered photons). The yield maximum determines the direction of planes and axes within the goniometer step width.

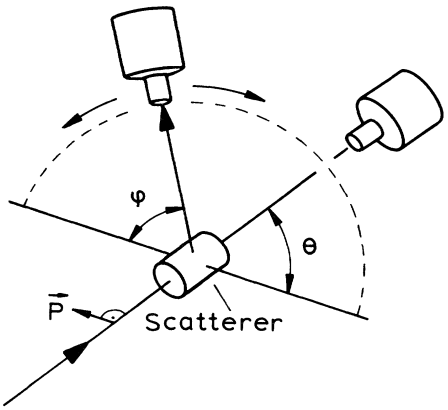

FIG. 2. Schematic view of the Compton scattering setup. The photon detector is mounted on a vertical turntable perpendicular ($\Theta=90°$) to the beam axis, such that any angle within the range of $\Delta\varphi=190°$ can be adjusted with an accuracy of 0.5°. φ is the detector azimuth with respect to the polarization plane indicated by the vector **P**. Also displayed is the position of the detector for the measurements of the energy spectra of unscattered photons with the scatterer removed.

B. Polarization analysis

The differential cross section for Compton scattering is described by the Klein-Nishina formula

$$\frac{d\sigma}{d\Omega}=\frac{r_0^2}{2}\left[\frac{E^2}{E_0^2}\right]\left[\frac{E}{E_0}+\frac{E_0}{E}-2\sin^2\Theta\cos^2\varphi\right], \quad (1)$$

where E_0 and

$$E=\frac{E_0}{[1+E_0/mc^2(1-\cos\Theta)]} \quad (2)$$

are the energies of the incident and scattered photon, respectively; r_0 is the classical electron radius, Θ the scattering angle and φ the azimuth of the scattering plane with respect to the polarization plane. In the energy range relevant for this experiment (50 to 200 keV) the lowest-order formula (1) agrees well with the experimental data and is adequate for polarization analysis. At $\Theta=90°$ the yield of photons scattered in the polarization plane ($\varphi=0°$) is very close to zero ($E/E_0+E_0/E\approx 2$), thus the analyzing power

$$A(E)=\frac{Y(\varphi=90°)-Y(\varphi=0°)}{Y(\varphi=90°)+Y(\varphi=0°)} \quad (3)$$

is of order unity. Here, $Y(\varphi)$ are the yields of 100% linearly polarized photons accepted by the polarimeter. The energy-dependent degree of the linear polarization $P(E)$ is the ratio of the experimental yield asymmetry and the analyzing power $A(E)$:

$$P(E)=\frac{1}{A(E)}\frac{Y_{\rm exp}(\varphi=90°)-Y_{\rm exp}(\varphi=0°)}{Y_{\rm exp}(\varphi=90°)+Y_{\rm exp}(\varphi=0°)} . \quad (4)$$

C. Monte Carlo simulation

The analyzing power $A(E)$ was determined by a detailed Monte Carlo simulation of the experiment[7] using the measured incident photon spectra and taking into account multiple Compton scattering as well as photoelectric absorption in the polyethylene scatterer. Since background contributions to the measured spectra are the dominating source of error, the geometry was optimized for maximum yields of scattered photons at the expense of analyzing power $A(E)$ and energy smearing due to angular acceptance and multiple Compton scattering which can be determined reliably by simulation. At $E_0=100$ keV the finally chosen polarimeter geometry resulted in an acceptance of 4.1×10^{-3} for unpolarized radiation, 22.2% multiple-scattering probability and an analyzing power $A=77.5\%$.

D. Background subtraction

In order to extract channeling radiation from the measured spectra (Fig. 3), background contributions due to bremsstrahlung in the crystal and other beam-related sources have to be removed. From each spectrum measured under channeling conditions a background spectrum taken with a crystal at random orientation was subtracted. In the forward direction the background contained in spectra measured under channeling conditions (Fig. 3, upper row) is entirely due to bremsstrahlung in the crystal. In the case of channeling along the silicon (110) plane the background amounts to 30% in the energy interval from 50 to 170 keV and to 27% in the energy interval from 50 to 250 keV in the case of the (110) plane of the diamond crystal. In contrast, the Compton scattered spectra (Fig. 3, lower row) contain substantial electron-beam-related background in addition to bremsstrahlung in the channeling crystal as is evidenced by the much stronger 511 keV annihilation line. The total background dominates the spectra measured at $\varphi=0°$ and thus determines the accuracy of the extracted Compton scattered channeling radiation yield. The background subtraction at $\varphi=0°$ is the most important error in the final polarization result (see below).

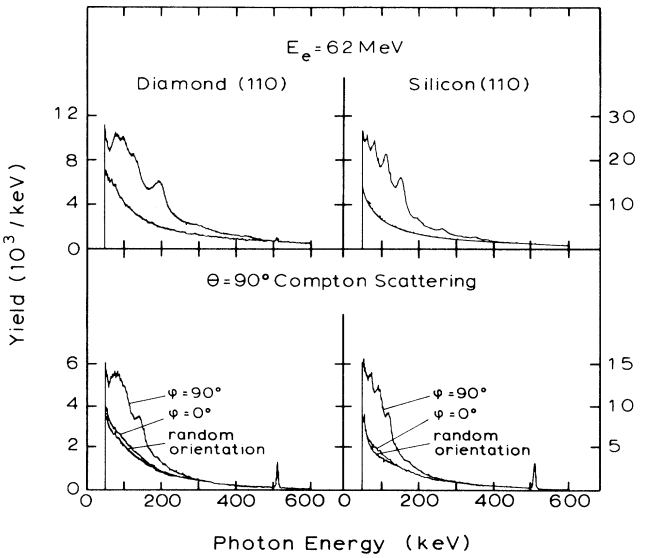

FIG. 3. Measured energy spectra of radiation emitted by 62 MeV electrons traversing a 50 μm thin diamond (left) and a 13 μm thin silicon (right) crystal; top row: forward channeling radiation in the (110) planes and bremsstrahlung for random orientations of both crystals; bottom row: $\Theta=90°$ Compton scattered planar channeling radiation for azimuths $\varphi=0°$ and 90°. Also displayed are Compton scattered spectra measured at $\varphi=0°$ with the crystals in random orientation.

In order to normalize channeling and bremsstrahlung spectra to each other two different methods were applied. Spectra measured in the forward direction were normalized by using the continuum yield above the 511 keV annihilation line which is free of channeling radiation (see Fig. 3), whereas Compton scattered spectra were normalized by the 511 keV line intensity which is due to high-energy background related to the electron beam. Generally, both methods agree within 1%. The intensities of the 511 keV line were measured with the crystals in channeling and in random orientations. No difference was observed within a statistical uncertainty of 3%. It was also ascertained that the shape of background spectra measured under $\Theta=90°$ with the polyethylene scatterer re-

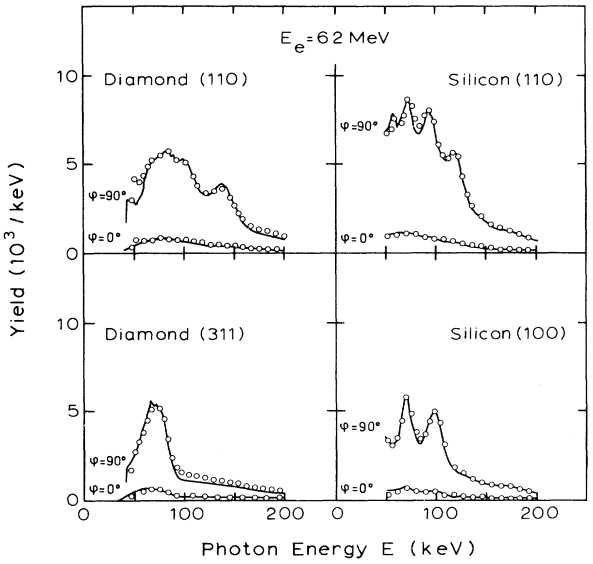

FIG. 4. Comparison of $\Theta=90°$ Compton scattered channeling radiation (azimuth $\varphi=0°$ and 90°) with Monte Carlo simulation results for 100% linearly polarized channeling radiation (polarization plane at $\varphi=0°$) for the (110) planes of diamond and silicon (top row) and the (311) plane of diamond and the (100) plane of silicon (bottom row). Background as measured with the crystals in random orientation is subtracted. The energy E is the photon energy after 90° Compton scattering.

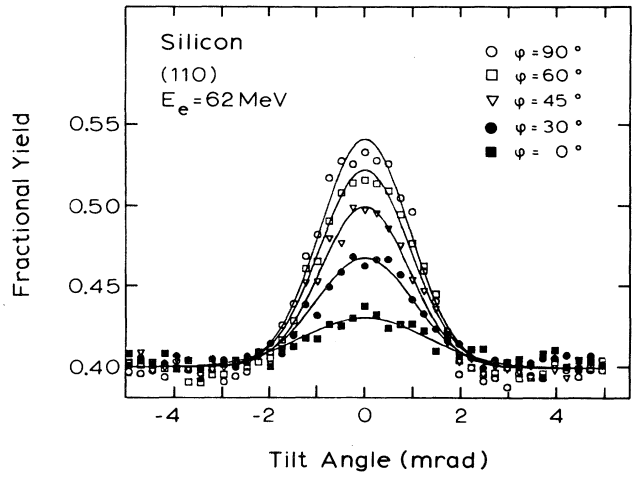

FIG. 5. Angular scans across the (110) plane of silicon. For various detector azimuths φ fractional yields of $\Theta=90°$ Compton scattered radiation within the energy window containing the main transition energies ($65<E<140$ keV) are displayed as a function of the crystal tilt angle. The curves are Gaussians fitted to the experimental data.

moved did not depend on the crystal orientation. For polarization analysis channeling radiation intensities scattered under different azimuths φ have to be compared to each other. Also for this purpose the Compton scattered spectra were normalized with respect to the intensity of the 511 keV line. Here, the separately measured φ dependence of background rates had to be taken into account.

Figure 4 shows channeling radiation spectra for the (110) and (311) planes of diamond and for the (110) and (100) planes of silicon at azimuthal angles $\varphi=0°$ and 90° after background subtraction. The measured spectra are in very good agreement with the Monte Carlo simulation of the experiment for 100% linearly polarized channeling radiation. The spectra at $\varphi=0°$ are dominated by multiple Compton scattering, therefore individual transition lines can no longer be resolved.

IV. RESULTS

A. Planar channeling

In Fig. 5 results of angular scans across the (110) plane in silicon are given. For various detector azimuths φ, fractional yields of Compton scattered radiation within the energy window containing the main channeling radiation lines ($65<E<140$ keV) are displayed as a function of the crystal tilt angle. For tilt angles larger than about 2 mrad only unpolarized bremsstrahlung is produced the scattering of which does not depend on φ. Approaching the (110) plane leads to an enhanced intensity due to channeling radiation and a strong φ dependence as expected for linearly polarized radiation.

In Fig. 6 the azimuthal distribution of the Compton scattered integral channeling radiation intensity ($50<E_0<400$ keV) is shown for the aligned silicon (110) plane and compared to simulation results for various degrees of linear polarization P. A fit to the experimental data results in $P=(97.6\pm4.0)\%$ and $\varphi_0=(1.1\pm1.4)°$, i.e., the radiation is completely linearly polarized over the entire energy spectrum and the polarization plane coincides with the normal to the channeling plane ($\varphi=0°$) as expected for planar channeling radiation. For diamond

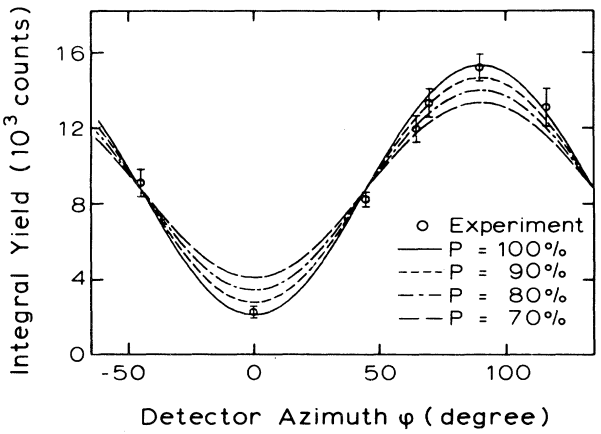

FIG. 6. Azimuthal distribution of the integral yield of $\Theta=90°$ Compton scattered channeling radiation for the (110) plane of silicon. The curves give simulation results for various degrees of linear polarization P assuming the normal to the (110) plane to be the polarization plane.

the average degree of linear polarization within the same energy interval is $P=(98.9\pm4.2)\%$ as determined from spectra measured at $\varphi=0°$ and 90°.

The energy dependence $P(E)$ of the degree of linear polarization of planar channeling radiation was extracted from Compton scattered spectra measured at $\varphi=0°$ and 90° for the (100) and (110) planes in silicon and for the (100), (110), (111), (211), and (311) planes in diamond. Results are shown in Fig. 7 for the (110) and (311) planes in diamond and for the (110) and (100) planes in silicon. Indicated are the energies corresponding to transitions between the lowest-lying bound states. As can be seen from Fig. 7, the channeling radiation for all planes is completely linearly polarized. In particular, also the continuum due to transitions involving unbound states is as strongly polarized as the indicated bound state transitions.

The error bars show representative 1σ errors composed of statistical and systematic contributions added in quadrature. The statistical error results from counting statistics of all six experimental spectra necessary to determine $P(E)$, i.e., from one spectrum each for channeling and random crystal orientations, for forward channeling radiation and for 90° scattering at $\varphi=0°$ and 90°. The statistical error varies between less than 1% and about 6%. The systematic error is due to positioning errors and absorption length uncertainties of the polyethylene target (all less than 0.6%) and systematic uncertainties introduced by normalizing the various experimental spectra to each other. Normalization errors are largest (up to 11%) for Compton scattered yields at $\varphi=0°$ where the signal to background ratio is small.

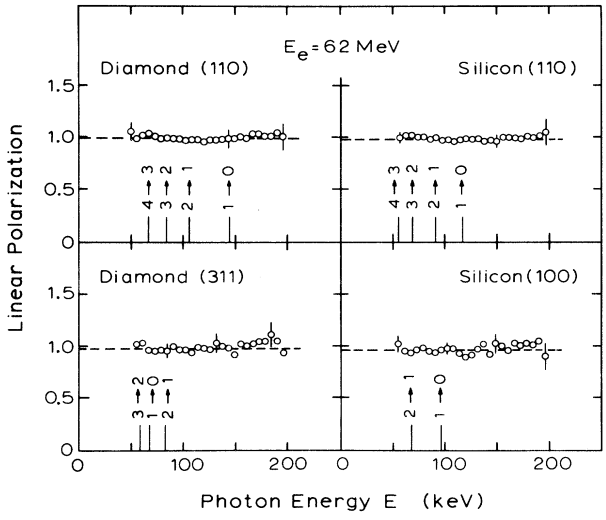

FIG. 7. Energy dependence of the degree of linear polarization $P(E)$ of planar channeling radiation for the (110) planes of both crystals (top row) and the (311) plane of diamond and the (100) plane of silicon (bottom row). The vertical lines indicate the energies corresponding to transitions between the lowest-lying bound states. The error bars give representative 1σ errors composed of statistical and systematic contributions added in quadrature. The horizontal dashed line corresponds to the average polarization over the entire energy range.

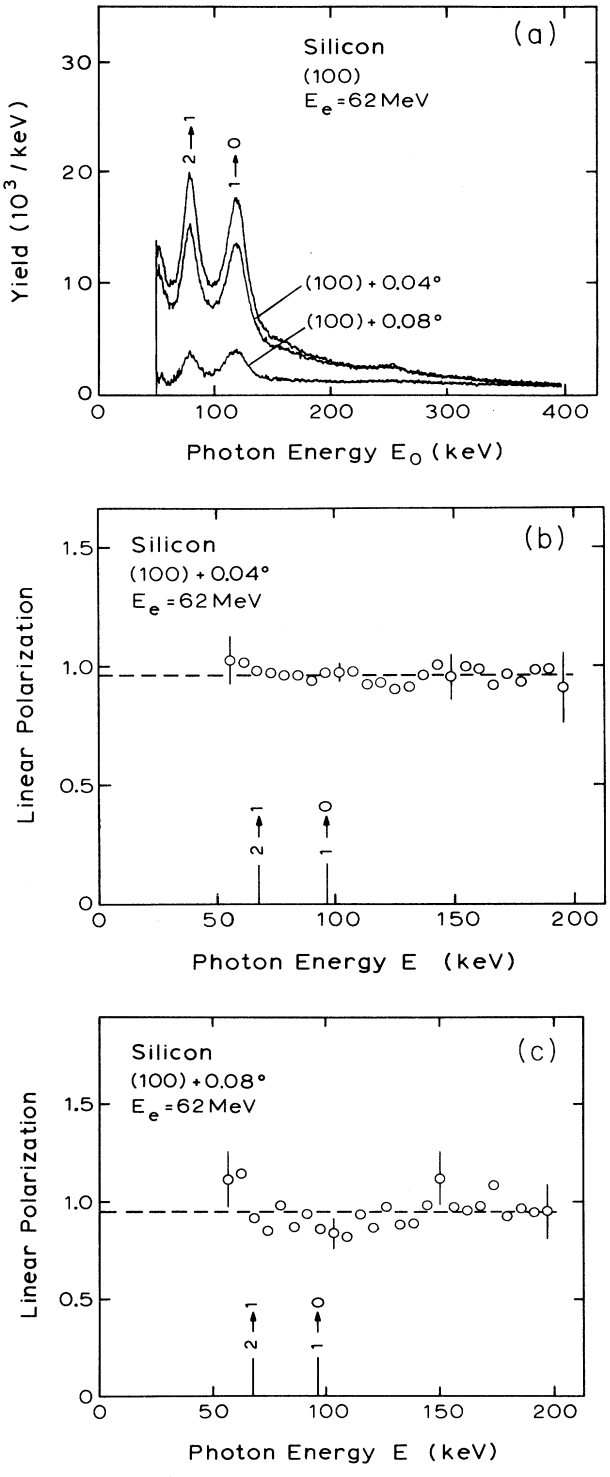

FIG. 8. Planar channeling radiation spectra and linear polarization for slightly different silicon crystal orientations. (a) Forward energy (E_0) spectra after bremsstrahlung subtraction for a precisely oriented (100) plane and two slightly (by 0.04° and 0.08°) tilted orientations in silicon. Two bound state transitions are indicated. The tilt increases the continuum due to transitions involving unbound states with respect to the intensity of the bound state transitions. (b) and (c) Energy dependence of the linear polarization (as Fig. 7) for the tilted crystal.

In order to enhance the continuum contribution to the channeling radiation spectra measurements were made with the silicon crystal slightly tilted [0.04° and 0.08° with respect to the direction of the (100) plane]. A small tilt angle of the order of the critical channeling angle will favor the population of unbound states compared to lower-lying bound states.[7] The experimental spectra [Fig. 8(a)] show reduced line intensities and enhanced continuum contributions for the tilted crystal, as expected. Combined fits of Lorentz-shaped lines together with third-order polynomials for the continuum reveal that the contribution of continuum transitions increases from 19% in the exact (100) direction to 35% for a tilt of 0.08° corresponding to slightly more than twice the critical channeling angle. Polarization analysis of spectra taken with the tilted silicon crystal [Figs. 8(b) and 8(c)] again leads to complete linear polarization within larger errors due to the reduced signal to background ratio.

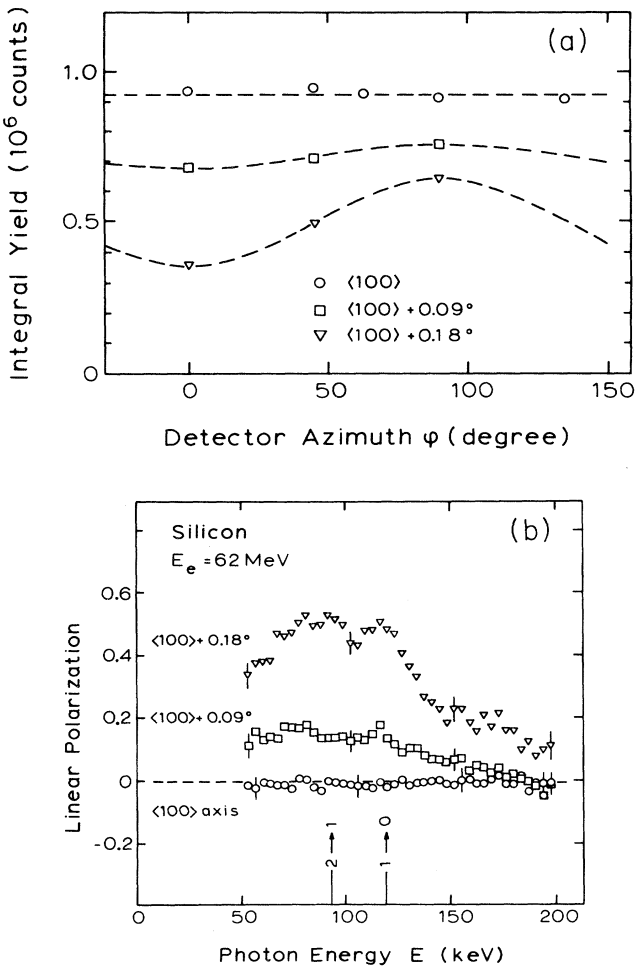

FIG. 9. (a) Azimuthal distributions of the integral yield of $\Theta = 90°$ Compton scattered axial channeling radiation produced with the silicon ⟨100⟩ axis exactly aligned (circles) and for two different tilt angles (0.09° and 0.18°) in the (110) plane. The curves show fits of $\cos^2\varphi$ distributions to the data. (b) Energy dependence of the linear polarization of axial channeling radiation for the ⟨100⟩ axis exactly aligned (circles) and tilted by 0.09° and 0.18°.

B. Axial channeling

Axial channeling was studied along the ⟨100⟩ axis in silicon. In addition to spectra taken with the axis exactly aligned with the incident electron direction, measurements were made with the crystal slightly tilted. In order to study the transition from axial to planar channeling tilt angles towards the (110) plane of 0.09° (slightly larger than the critical channeling angle of the ⟨100⟩ axis) and 0.18° were chosen. Results are given in Fig. 9. The Compton scattered integral yield [Fig. 9(a)] for the exact axis orientation does not depend on the azimuth φ as expected for unpolarized radiation. For a tilt angle of 0.09° a slight and for 0.18° a substantial linear polarization is observed. The polarization plane coincides with the normal to the (110) plane, demonstrating that the channeling radiation produced with the tilted crystal is a superposition of axial and planar channeling contributions. This is further substantiated by the spectral distribution $P(E)$ of the degree of linear polarization [Fig. 9(b)]. For the exact axis orientation $P(E)$ is zero everywhere in the energy interval covered. With increasing crystal tilt linear polarization builds up with maximum values reaching as much as 50% for 0.18° at energies corresponding to the discrete lines of planar channeling radiation at the (110) plane.

V. DISCUSSION AND SUMMARY

We have studied the linear polarization of planar and axial channeling radiation in the energy range from 50 to about 400 keV produced by 62 MeV electrons incident on a 13 μm thin silicon and a 50 μm thin diamond crystal. Planar channeling radiation due to transitions between transverse bound as well as unbound states is completely linearly polarized perpendicular to the channeling plane. This is as expected for pure dipole radiation in spontaneous transitions between energy levels of the one-dimensional continuum potential used in the many-beam formalism[3] to approximate the three-dimensional lattice potential. The measured linear polarization thus renders additional support to this continuum approximation which has been successfully applied to calculate channeling radiation energy spectra. Axial channeling radiation produced along the ⟨100⟩ axis in silicon does not show linear polarization, again in accord with expectations for an azimuthally symmetric two-dimensional potential of a continuous string of charges. Channeling radiation produced with the ⟨100⟩ axis slightly rotated within the (110) plane in silicon is linearly polarized to an extent consistent with being a simple superposition of unpolarized axial and completely polarized planar channeling radiation. The off-axis polarization data thus do not give any hint to qualitatively new radiation phenomena in the transition from axial to planar channeling radiation, as may have been suggested in previous measurements of energy spectra.[15] Also, the experimental results do not support model calculations[8] following the many-beam approach which predict substantial linear polarization

(around 50%) for tilt angles in the order of the critical axial channeling angle.

Our polarization measurements establish planar channeling radiation as a useful tunable narrow band source of highly polarized x rays. The effective degree of linear polarization is simply given by the fractional contribution of channeling radiation to the total intensity composed of 100% linearly polarized channeling radiation and unpolarized bremsstrahlung. The polarization plane can be chosen by appropriate crystal orientation. We have already made use of planar channeling radiation of a beryllium crystal to develop a polarimeter based on the photoeffect.[16]

ACKNOWLEDGMENTS

This work was supported by the German Federal Minister for Research and Technology (BMFT) under Contract No. 06DA665I. The authors wish to thank the S-DALINAC group at Darmstadt, in particular H.-D. Gräf and E. Spamer, for the operation of the accelerator and for technical support and the technical staff of the Max-Planck Institut für Physik, in particular W. Erbe, for their contributions to the construction and installation of the experiment. The MPI authors gratefully acknowledge the hospitality extended to them at the Institut für Kernphysik at Darmstadt.

[1]M. A. Kumakhov, Phys. Lett. **57A**, 17 (1976).

[2]B. L. Berman and S. Datz, in *Coherent Radiation Sources,* edited by A. W. Sáenz and H. Überall (Springer, Berlin, 1985), p. 165.

[3]J. U. Andersen, E. Bonderup, E. Lægsgaard, B. B. Marsh, and A. H. Sørensen, Nucl. Instrum. Methods Phys. Res. **194**, 209 (1982).

[4]M. A. Kumakhov, Phys. Status Solidi B **84**, 41 (1977).

[5]J. U. Andersen, E. Bonderup, E. Lægsgaard, and A. H. Sørensen, Phys. Scr. **28**, 308 (1983).

[6]A. W. Sáenz, H. Überall, and A. Nagl, Nucl. Phys. **A372**, 90 (1981).

[7]M. Rzepka, Ph.D. thesis, Technische Universität, München, 1994.

[8]R. Fusina, Phys. Rev. B **42**, 7706 (1990).

[9]Yu. N. Adishchev, I. E. Vnukov, S. A. Vorob'ev, V. M. Golovkov, V. N. Zabaev, V. I. Lunev, A. A. Kurkov, B. N. Kalinin, and A. P. Potylitsyn, JETP Lett. **33**, 462 (1981).

[10]Yu. N. Adischev, R. D. Babadjanov, I. E. Vnukov, A. P. Potylitsyn, and I. Khakberdiev, Radiat. Eff. **91**, 217 (1986).

[11]E. Diedrich, G. Buschhorn, W. Kufner, M. Rzepka, H. Genz, H.-D. Gräf, P. Hoffmann-Stascheck, and A. Richter, Phys. Lett. A **178**, 331 (1993).

[12]P. Hoffmann-Stascheck (unpublished).

[13]M. Rzepka, G. Buschhorn, E. Diedrich, R. Kotthaus, W. Kufner, W. Rössl, K. H. Schmidt, H. Genz, H.-D. Gräf, P. Hoffmann-Stascheck, and A. Richter, Nucl. Instrum. Methods Phys. Res. Sect. B **90**, 186 (1994).

[14]J. Auerhammer, H. Genz, H.-D. Gräf, R. Hahn, P. Hoffmann-Stascheck, C. Lüttge, U. Nething, K. Rühl, A. Richter, T. Rietdorf, P. Schardt, E. Spamer, F. Thomas, O. Titze, J. Töpper, and H. Weise, Nucl. Phys. **A553**, 841c (1993).

[15]E. Diedrich, G. Buschhorn, W. Kufner, M. Rzepka, H. Genz, P. Hoffmann, U. Nething, and A. Richter, Nucl. Instrum. Methods Phys. Res. Sect. B **67**, 275 (1992).

[16]G. Buschhorn, R. Kotthaus, W. Kufner, W. Rössl, M. Rzepka, K. H. Schmidt, H. Genz, H.-D. Gräf, P. Hoffmann-Stascheck, U. Nething, A. Richter, W.-R. Dix, G. Illing, M. Lohmann, J. Pflüger, R. Reime, and L. Schildwächter, Nucl. Instrum. Methods Phys. Res. Sect. A **346**, 578 (1994).